Modeling Wrinkles on Smooth Surfaces for Footwear Design

Fu Jing[1], Ajay Joneja[2] and Kai Tang[3]
[1]HK University of Science & Technology, fujing@ust.hk
[2]HK University of Science & Technology, joneja@ust.hk
[3]HK University of Science & Technology, mektang@ust.hk

ABSTRACT

We describe two new shape operators that superimpose wrinkles on top of a smooth NURBS surface. Previous research studying wrinkles focused mostly on cloth modeling or in animations, which are driven more by visual realism, but allow large elastic deformations. Our operators generate wrinkle-shaped deformations in a region of a smooth surface along a given boundary based on a few basic parametric inputs such as wrinkle magnitude and extent (these terms will be defined in the paper). The essential geometric transformation to map the smooth surface to a wrinkled one will be defined purely in terms of the geometry of the surface and the input parameters. Our model is based on two surface properties: geodesic offsets and surface energy. Practical implementation of the operators is discussed, and examples presented. Finally, the motivation for the operators will be given through their application in the computer-aided design and manufacture of footwear.

Keywords: Wrinkles, Geodesic curves, Geodesic offsets, Surface energy, CAD

1. INTRODUCTION

The objective of this paper is to develop shape operators that superimpose a wrinkle shape onto a given smooth surface. Such an operator has some practical interest, especially in the Computer-Aided Design (CAD) of textiles and footwear. Most recent research in study of wrinkling of flexible, sheet-like materials has been related to textiles. The models attempt to predict the shape that a given piece of textile, in the form of a 2D shape *pattern*, will take when draped over a particular solid form at a given position. The resulting shape is a possibly wrinkled 3D surface. The main successful studies used tessellated approximations of the pattern, imposed boundary conditions based on the 3D form over which the textile is draped, and used finite element techniques to iteratively compute the equilibrium state of the pattern. Gravitational and even inertial forces can be incorporated into such models. An older survey of such modeling techniques can be found in [1], with more recent research being reported in [2, 3, 4, 5]. A general shape deformation operator tool that could also be used to define wrinkles was discussed in [6]. It uses the notion of *wire* deformations as follows: a wire is a smooth curve, $\boldsymbol{c}(t)$, with a radius function $r(t)$ associated with each point. Each point on a given surface $\boldsymbol{S}(u, v)$ in the interior of the canal surface (see [7] for description of canal surfaces) formed by $r(t)$ and $\boldsymbol{c}(t)$ is transformed by a wire deformation according to (i) its weight, which is a typically a smooth function of its Euclidean distance from $\boldsymbol{c}(t)$, and (ii) the deformation of the wire curve, $\boldsymbol{c}(t)$, made by the user. Since the deformations can be arbitrary, this is a generic tool without any particular insight into the physical process of deformations in general, and wrinkling in particular.

Our interest is specifically in the CAD of footwear. The manufacture of shoes begins with a plastic (or wooden) mold called the shoe last. The shoe upper is wrapped tightly around the shoe last (see Figure 1), and then glued to the sole to form the shoe shape. Using CAD technology, the first step is to define the shape of the shoe last; a surface offset operation is then used to create the geometry of the shoe upper. However, while the surface of the shoe last is mostly smooth, it is often desirable that some regions of the shoe upper are wrinkled (e.g., see Figure 2). This requirement is sometimes driven by aesthetic (i.e., design-driven) requirements, and at other times due to manufacturing requirements. The last, and its CAD model, are made up of smooth surfaces; by offsetting [8] these surfaces by the thickness of the leather, we can obtain the approximate surface geometry of the shoe upper. This model, however, is smooth. It is possible for the designer to directly manipulate the geometry of the surface in order to create wrinkles. However, this would involve

tedious steps such as inserting several new points in the control mesh, and manually moving them around until the desired shape is created. Another issue in footwear design is that the upper is created by stitching together several flat pieces of leather (or synthetic material). The raw materials are essentially flat. On the other hand, the shape of the shoe last is curved in such a way that wrapping the upper forces the relatively inelastic leather to wrinkle in some regions. These wrinkles can sometimes be covered (e.g. the region that is glued to the sole), and at other times be ironed out after the shoe is manufactured. Suppose that the geometry of the 2D patterns required to create the upper is generated by applying a surface development algorithm [9, 10, 11] to the offset surface of the last. The resulting patterns will be inaccurate since they do not realistically allow for the wrinkling allowed on the real uppers.

To cater to these requirements, we study the form of the wrinkles in the prescribed setting and provide a practical tool for creating the desired wrinkles by offering two new shape modification operators. The first is a parametric wrinkle operator that allows the designer to manipulate the geometry of the wrinkles in terms of a set of simple parameter values. The second wrinkle operator uses the surface energy of the region of the wrinkle's extent to determine the frequency and the shape of the wrinkles. We are not aware of any past research studying such shape modification operations to create wrinkles on a specified region of a given smooth surface.

Fig. 1. A shoe last

Fig. 2. A Shoe with designed wrinkles

2. PROBLEM STATEMENT

Two different models for wrinkles are presented in the following sections. We first give a somewhat informal description of the corresponding problem statements in this section.

Parametric wrinkle operator:
We are given a smooth B-Spline (or NURBS) surface $\boldsymbol{S}$, and a curve $\boldsymbol{C}$ lying on it. The wrinkle is defined in terms of parameters that control its boundary conditions and the extent (to be defined below). The boundary conditions define the maximum amplitude, a, of the wrinkle normal to its boundary at $\boldsymbol{C}$. The extent of the wrinkle defines the region on S that will be affected by the wrinkle. The extent, e, is the distance measured along the surface, starting orthogonal to the boundary curve $\boldsymbol{C}$, and moving along the geodesic from each point on $\boldsymbol{C}$. The designer can control the frequency of the wrinkles by specifying the number of wrinkles, n, to be created along $\boldsymbol{C}$. The objective is to define a wrinkle dislocation function $\boldsymbol{w}(u,v)$ that generates, for each point (u,v) on $\boldsymbol{S}$, the displacement vector due to the wrinkling. In practice, we shall compute a series of points using the function $\boldsymbol{w}(u_i, v_j)$, $i = 1, 2,\ldots, N$ and $j = 1, 2,\ldots, M$ for some suitably large N and M. This discrete set of points will be used to generate the wrinkles on the surface.

Surface Energy Based Wrinkle Operator:
In footwear/clothing manufacturing, we are often given a region on a smooth mold, over which a flexible but relatively inelastic pattern must be draped. The region is specified as before, by the generator curve C and extent e. If the surface is non-developable, then the pattern will wrinkle. In this case, the objective is to minimize the wrinkling, since it results in a minimum area pattern required to completely drape the specified region of the surface. For this operator, a measure of the surface energy (integral of the Gaussian curvature over the surface) is used to determine the magnitude of the wrinkle. An optimization model incorporating geometric and physical constraints is developed to generate the required wrinkle geometry.

3. PARAMETRIC WRINKLE OPERATOR

In this section, we describe in detail the first of the two wrinkle operators, which will also be the basis for the second and more enhanced operator. Several wrinkle forms were studied via a series of simple examples using leather-like materials (a few examples are shown in Figure 3). Inspired by these physical models, the model for our operator is then developed in terms of three aspects: (a) the dislocation of the wrinkled form from the

mold surface at the boundary; this is the region where the dislocation is maximum; (b) the direction along which the wrinkle propagates along the mold surface; and (c) the region covered by the wrinkles, i.e. the extent. Figure 4 illustrates these three aspects. We note here that there appears to be a stochastic element to wrinkle behavior, which though is ignored in our models.

Fig 3(a) Image, spherical mold

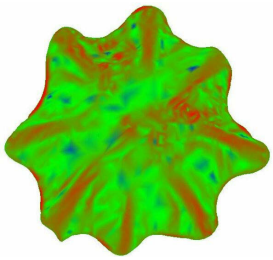

Fig 3(b). Model from CMM scan

Fig. 3(c). Image, ellipsoidal mold

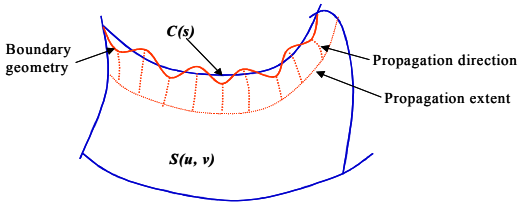

Fig. 4. Basic wrinkle model

Let $\boldsymbol{S}(u,v)$ be the given surface, and $\boldsymbol{C}(s)$, $0 \le s \le L$, be the curve defined on it as the boundary curve of the wrinkles. For notational simplicity, we assume that s is the natural parameter (arc length). The boundary dislocation due to the wrinkle is modeled as a displacement normal to the surface, explicitly as a sinusoidal function given by:

$$w(s) = a\ \boldsymbol{sin}\left(2\frac{s}{L}\pi n\right) N\ ,$$

where and $\boldsymbol{S}_u$ and $\boldsymbol{S}_v$ are the partial derivatives of the surface with respect to the parameters u and v at point $\boldsymbol{C}(s)$. This generates the specified number, n, of waveforms along $\boldsymbol{C}$. The next issue is to propagate the wrinkles along the surface of the mold. Based on our experimental data, a reasonable choice is to let the winkle deformations travel along the surface perpendicular to $\boldsymbol{C}$ initially, propagating along geodesics on the surface. As the wrinkle travels away from the boundary, the amplitude of $\boldsymbol{w}(s)$ diminishes smoothly to zero as the geodesic distance traversed equals the extent e. In our case, we adopt a simple linear decay function. Here we emphasize that since most wrinkle forms actually lose contact from the mold surface, any model based on the mold surface is only realistic over small and relatively smooth regions (i.e. for relatively small wrinkles). In terms of computing geodesic curves on a surface [12], several researchers have studied this problem in other contexts earlier, for example, refer to [13, 14, 15, 16]. We describe the basics and our algorithm for these computations next.

The curvature at a point on the surface $\boldsymbol{S}$ is given by $\boldsymbol{k} = (\boldsymbol{k}.\boldsymbol{U})\boldsymbol{U} + (\boldsymbol{k}.\boldsymbol{N})\boldsymbol{N}$, where $\boldsymbol{U} = \boldsymbol{N} \times \boldsymbol{C'(s)}$, and $\boldsymbol{N}$ is the surface normal. For a geodesic, the first term $(\boldsymbol{k}.\boldsymbol{U})\boldsymbol{U}$ vanishes. Further, if $\boldsymbol{E1}$, $\boldsymbol{E2}$ form a frame field on $\boldsymbol{S}$, then the coefficients of both terms of its acceleration,

$$\boldsymbol{C''} = \left(u'' + \frac{1}{2}\boldsymbol{E}\left(\boldsymbol{E}_u u'^2 + 2\boldsymbol{E}_v u'v' + \boldsymbol{G}_u v'^2\right)\right)\boldsymbol{E}_1 +$$

$$\left(v'' + \frac{1}{2}\boldsymbol{G}\left(-\boldsymbol{E}_v u'^2 + 2\boldsymbol{G}_u u'v' - \boldsymbol{G}_v v'^2\right)\right)\boldsymbol{E}_2$$

must vanish locally, where $\boldsymbol{E}$, $\boldsymbol{F}$, $\boldsymbol{G}$ are the inner products, $\boldsymbol{E} = \langle \boldsymbol{S}_u, \boldsymbol{S}_u \rangle$, $\boldsymbol{F} = \langle \boldsymbol{S}_u, \boldsymbol{S}_v \rangle$ and $\boldsymbol{G} = \langle \boldsymbol{S}_v, \boldsymbol{S}_v \rangle$; thus:

$$u'' + \tfrac{1}{2}\boldsymbol{E}\left(\boldsymbol{E}_u u'^2 + 2\boldsymbol{E}_v u'v' + \boldsymbol{G}_u v'^2\right) = 0,$$

and

$$v'' + \tfrac{1}{2}\boldsymbol{G}\left(-\boldsymbol{E}_v u'^2 + 2\boldsymbol{G}_u u'v' - \boldsymbol{G}_v v'^2\right) = 0.$$

Any of the several known numerical methods to solve systems of differential equations may be used here [13, 16]; we used a simple iterative algorithm based on Euler's technique to generate geodesics. The algorithm computes an approximate geodesic by starting to move orthogonal to the boundary curve $\boldsymbol{C}$, taking tiny steps along the geodesic at each point. At each step, the algorithm performs three actions: (i) computes the direction in which to move; (ii) moves to a point a short

distance along the surface tangent in this direction; and (iii) projects this point onto the surface $\boldsymbol{S}$. If the projection distance is larger than an acceptable tolerance, the step size is adaptively reduced and the procedure repeated.

There are two cases to consider in determination of the direction of move at each step. From the initial point, $\boldsymbol{C_0}$ on $\boldsymbol{C}$, the first step is along the direction orthogonal to the curve tangent $\boldsymbol{C'_0}$, on the tangent plane at $\boldsymbol{C_0}$, which is along the vector $\boldsymbol{C'_0 \times N_0}$ (Figure 5), where $\boldsymbol{N_0}$ is the surface normal at $\boldsymbol{C_0}$. From an intermediate point, $\boldsymbol{C_i}$, the direction is determined based on the fact that the three vectors, $\boldsymbol{C_i - C_{i-1}}$, $\boldsymbol{C_{i+1} - C_i}$, and the surface normal $\boldsymbol{N_i}$ at $\boldsymbol{C_i}$, must be co-planar. Thus the step is along the direction $(\boldsymbol{N_i \times (N_i \times (C_i - C_{i-1})})$. The projection of the initial point on to the surface (e.g., the projection of $\boldsymbol{C^*_1}$ to $\boldsymbol{C_1}$ in Figure 6 below) is performed using a standard Newton-Raphson numerical procedure.

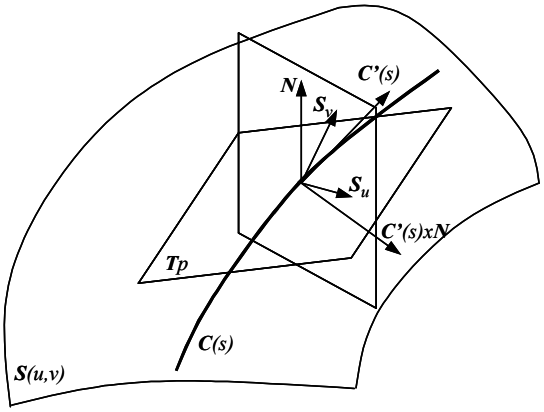

Fig. 5. Geodesic lies on the normal plane

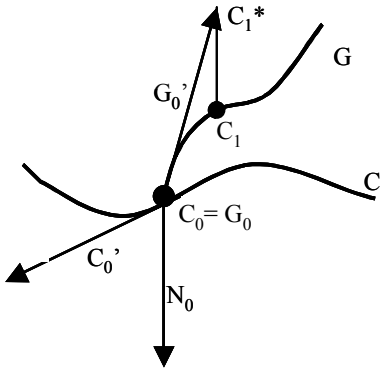

Fig. 6. Computing C_1 from $\boldsymbol{C_0}$

A practical issue arises when the geodesic curve must move across the boundary of one patch onto another path on a composite surface. In general, the surface may not be C^1 continuous at this boundary. Figure 7 shows how this is handled in our model. Here we assume that the two surfaces, $\boldsymbol{S_1}$ and $\boldsymbol{S_2}$ meet along a curve $\boldsymbol{C}$. The current point $\boldsymbol{C^*_i}$ on the geodesic curve $\boldsymbol{G}$ on $\boldsymbol{S_1}$ is discovered to lie outside $\boldsymbol{S_1}$ (that has been trimmed by $\boldsymbol{S_2}$). We first shorten the step size, using bisection method, so that the current point $\boldsymbol{C_i}$ lies on curve $\boldsymbol{C}$. The subsequent point, $\boldsymbol{C_{i+1}}$, will then lie on surface $\boldsymbol{S_2}$. We first obtain $\boldsymbol{C^*_{i+1}}$, which is computed by moving a distance δ along direction $\boldsymbol{d}$ on the tangent plane at $\boldsymbol{C_i}$ on $\boldsymbol{S_2}$. The direction is obtained by the following relationship:

$$\frac{C_i - C_{i-1}}{|C_i - C_{i-1}|} \cdot (\boldsymbol{t} \times \boldsymbol{n}_1) = \boldsymbol{d} \cdot \boldsymbol{t}$$

where $\boldsymbol{t}$ is the unit tangent vector to $\boldsymbol{C}$ at $\boldsymbol{C_i}$, and $\boldsymbol{n}_k$ are the unit normal vectors to $\boldsymbol{S}_k$ ($k = 1, 2$) at $\boldsymbol{C_i}$. $\boldsymbol{C_{i+1}}$ is then found by projecting $\boldsymbol{C^*_{i+1}}$ onto S2 as before.

Using the above procedures, it is possible to (a) define the wrinkle deformation at any point on $\boldsymbol{C}$, and (b) by moving along the geodesic orthogonal to $\boldsymbol{C}$ from the selected point, it is possible to generate the wrinkle displacement at any point $\boldsymbol{P}$ on the geodesic curve as $w = \frac{(e - s_g)}{e} a \sin(2\frac{s}{L}\pi n) N$, where s_g is the arc length of the geodesic from $\boldsymbol{C_0}$ to $\boldsymbol{P}$, and $\boldsymbol{N}$ is the unit surface normal at $\boldsymbol{P}$.

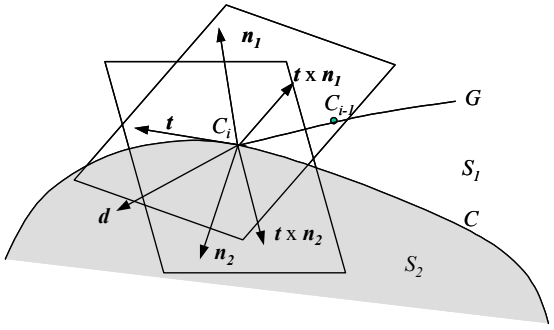

Fig. 7. Geodesic across neighboring patches

Fig. 8. Shoe upper

Fig. 9. Wrinkled shoe upper *n=10, e=10, a=2*

Although we use a sinusoidal form to generate the wrinkle deformation and superimpose it onto the original smooth surface, it is sometimes convenient to define the wrinkled surface itself as single a B-Spline surface. One may generate the wrinkle deformation for a large number of points, and then interpolate a B-Spline surface through these points [17]. Another option is to create a series of diminishing wave-like forms along geodesic offset contours in the wrinkle region, and then fit a skinned surface [17] through these points. Figure 8 shows a pattern for a shoe upper, and Figure 9 shows wrinkles superposed along a portion of its boundary using the above model.

4. SURFACE ENERGY-BASED WRINKLES

While the parametric wrinkle operator described in the preceding section provides a basic and convenient tool for wrinkle design, in this section, we present an enhanced model for wrinkles, based on surface energy redistribution. The goal is to achieve realistic wrinkling of a flexible, flat pattern that is forced to drape over a non-developable mold surface.

4.1 Basic description of the operator

The surface energy of a thin sheet is given by $E_{surface} = \iint a(\kappa_1^2 + \kappa_2^2) + 2(1-b)\kappa_1\kappa_2 dS$, where κ_1 and κ_2 are the principal curvatures and a and b are controlling weights. The first term in the integral estimates the bending energy, while the second term pertains to the intrinsic energy. To model wrinkles, we ignore the first term, since (a) pure bending can be achieved without wrinkling, and (b) bending energy is low for flexible materials such as textiles and leather. The second term is a function of the Gaussian curvature, $K = \kappa_1 \kappa_2$. The proposed model is based on the assumption that the amplitude of the wrinkling is proportional to the integral of the Gaussian curvature over the wrinkling region. In order to establish a gross measure, the absolute value should be used, i.e., $E_{wrinkling} \propto \int |k_1 k_2| dS = \int |K| dS$. It is though difficult to evaluate this surface integral directly; so we invoke the Gauss-Bonet theorem [12]. Let $\boldsymbol{S}$ be an oriented, smooth surface and R be a simple region of $\boldsymbol{S}$. $\alpha: I \rightarrow \boldsymbol{S}$ such that $\partial R = \alpha(\mathrm{I})$. Assume that α is positively oriented, parameterized by arc length s, and let $\alpha(s_0), \ldots, \alpha(s_k)$ and $\theta_0, \ldots, \theta_k$ be, respectively, the vertices and the external angles of α. Then

$$\sum_{i=0}^{k} \int_{S_i}^{S_{i+1}} \kappa_g(s) ds + \iint_R \mathrm{K} d\sigma + \sum_{i=0}^{k} \theta_i = 2\pi ,$$

where $\kappa_g(s)$ is the geodesic curvature of the regular arcs of α and K is the Gaussian curvature of R. In particular, consider a four-sided patch on the surface of the form as shown in Figure 10.

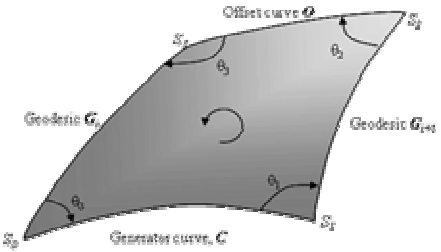

Fig. 10. Four-sided patch bounded by boundary curves and geodesics

For the two geodesics, $\kappa_g = 0$ and $\theta_0 = \theta_1 = \pi/2$, so

$$\iint_R \mathrm{K} d\sigma = \pi - \theta_2 - \theta_3 - \int_{S_0}^{S_1} \kappa_g(s) ds - \int_{S_2}^{S_3} \kappa_g(s) ds$$

The θi are calculated by vector arithmetic, while a numerical approximation method is used to compute the integral of κ_g along the two non-geodesic boundary curves.

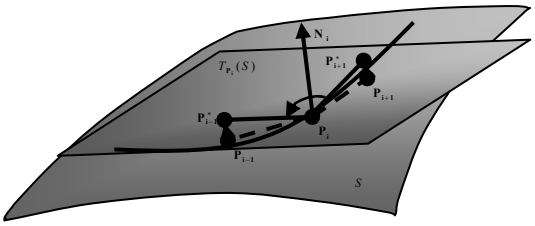

Fig. 11. Computing the surface curvature

Refer to Figure 11, for a sufficiently short, linear approximation of a curve $\mathbf{C}$, we get a sequence of vertices $\boldsymbol{P}_0, \ldots, \boldsymbol{P}_k$, and $\varphi(\mathbf{P}_i) = \angle \mathbf{P}^*_{i-1} \mathbf{P}_i \mathbf{P}^*_{i+1}$, where

$\boldsymbol{P}^*_{i-1}$ and $\boldsymbol{P}^*_{i+1}$ are respectively the projections of $\boldsymbol{P}_{i-1}$, $\boldsymbol{P}_{i+1}$ on the tangent plane of $\boldsymbol{S}$ at $\boldsymbol{P}_i$. Thus

$$\int_{S_a}^{S_b} k_g(s)ds = \sum_{i=a+1}^{b-1}(\pi - \varphi(\mathbf{P}_i))$$

.

There are two issues that remain to be resolved. Firstly, for a given region of the mold on which the leather will be draped, one or several wrinkles may form (as is Figure 3), merely getting a gross estimate of the energy over the entire region, as above, is not sufficient in estimating the amplitude and distribution. Secondly, if the curvature of the shape is distributed non-uniformly, then the wrinkles will not be uniformly distributed or of similar size. To account for these, we divide the entire wrinkle region into strips by means of a series of geodesic curves generated as follows. The wrinkle region is defined, as before, by specifying a generator curve, $\boldsymbol{C}$, and the extent. A sufficiently dense series of equi-spaced points is first generated along $\boldsymbol{C}$. From each of the points, we create a geodesic curve, starting initially perpendicular to $\boldsymbol{C}$. The length of each geodesic is equal to the specified extent. The end points of the geodesics are joined to form the wrinkle region. The energy for each strip is computed using the aforementioned method.

Each wrinkle is generated over one or a set of adjacent strips (see Figure 12), depending on the two factors: (a) the total energy of the set of strips is nearly equal to a specified threshold value, and (b) there is the possibility of constrained lateral shifting of the flexible material. The first factor essentially controls the number of wrinkles that will form over the surface. This depends not only on the surface properties, but also on the material properties (e.g., stiffness which is controlled by the threshold) of the leather. A suitable method to generate realistic wrinkles will entail some empirical work correlating material properties with their wrinkling behavior. The second factor accounts for the following: suppose we have a surface such that one paving is shaped to create a wrinkle, while its adjacent paving is tending to stretch the material. In such cases, some material shifts from the first paving to its neighbor, thereby reducing the tensile stress in the second paving and reducing the wrinkling in the first. However, such lateral shift of material is not completely unconstrained. Especially in textile and footwear manufacture, the flat pattern is first fixed along some profile, and then draped onto the region to be covered. This procedure only allows restricted amount of lateral shifting. We develop a model to simulate this situation.

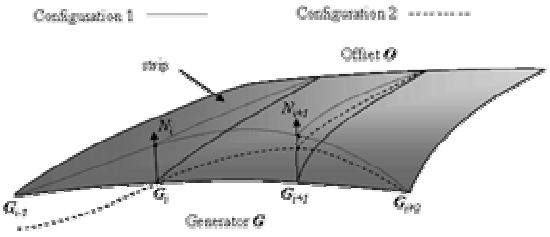

Fig. 12. Alternate wrinkle configurations

The amplitude of each wrinkle is controlled by the geometry of its corresponding patch. Two of the factors affecting it are the surface energy and the boundary lengths. Suppose the original length of the portion on curve with half wrinkle (one peak point) is L_G and the corresponding length is $L_{G'}$ after wrinkling; we adopt the sinusoidal model of section 3.1, i.e.,

$$w(s) = a\sin(\frac{s}{L_G}\pi)N$$

.

The final length of the boundary curve $L_{G'}$ will lead to the area increase in order to cover the non-developable surface. The area increase, proportional to the original area, can be approximated by $(L_{G'} - L_G)/(L_G + L_O)$, where L_O is the length of the patch boundary on the offset curve. A simple linear relationship between the integral of the Gaussian curvature, K^*, and the approximate area increase is proposed:

$$\frac{L_G' - L_G}{L_G + L_O} = \beta K^*,$$

where β is a positive coefficient and can be decided by the property of material. Now we can construct:

$$L_G' = \Phi(K^*, L_G, L_O) = \beta K^*(L_G + L_O) + L_G$$

All the variables in the above function can be provided or computed from the previous discussions, and the final length of the deformed boundary can be obtained according to the property of the surface. Once $L_{G'}$ is available, the amplitude a can be estimated by the equation below:

$$L_G' = \int\sqrt{1-(f'(s))^2}\,ds = \int_0^{L_G}\sqrt{1+\left[\frac{a\pi}{L_G}\cos(\frac{\pi}{L_G}s)\right]^2}\,ds$$

In our implementation, this is solved numerically using an iterative binary search.

4.2 Wrinkle Optimization for Minimum Material Requirement

Suppose that a region on a mold is prescribed, and we want to drape a sheet of certain material over it. If this region is non-developable, there will be some wrinkling; the orientation of the wrinkles is dictated by the

manufacturing application, and therefore, we subdivide the region into strips along this direction. Combining contiguous strips will define a paving, with one wrinkle per paving. Each wrinkle potentially uses more area of material than the area of the underlying paving. The extra material required can only come from "borrowing:" some material from the adjacent paving. This is true for all except the two extreme strips, which can borrow unlimited amount of material across their outer boundary.

In the previous section, we prescribe that the area added to generate a wrinkle is a function of boundary length together with the total curvature K^* of that region, say $L_{G'} = \Phi(K^*, L_G, L_0)$. Initially, we obtain n small stripes according to the method discussed before and the parameters as below:

$K^* = \{K_0^*, K_1^*, ...K_{n-1}^*\}$, $L^G = \{L_0^G, L_1^G, ...L_{n-1}^G\}$, and $L^O = \{L_0^O, L_1^O, ...L_{n-1}^O\}$.

A single paving, which includes one or more contiguous stripes, will contribute some increase of the area, as well as the length increase on the boundary. Suppose the paving is constructed by merging the stripes indexed from the i-th to the j-th, then:

$$K_{ij}^* = \sum_{k=i}^{j} K_k^*, \quad L_{ij}^G = \sum_{k=i}^{j} L_k^G, \quad L_{ij}^O = \sum_{k=i}^{j} L_k^O.$$

Let F_{ij} be the area increase in this region; we have

$$F_{ij} = \Phi(K_{ij}^*, L_{ij}^G, L_{ij}^O) = \Phi(\sum_{k=i}^{j} K_k^*, \sum_{k=i}^{j} L_k^G, \sum_{k=i}^{j} L_k^O).$$

In our model,

$$\Phi(K_{ij}^*, L_{ij}^G, L_{ij}^O) = \beta \sum_{k=i}^{j} K_k^* (\sum_{k=i}^{j} L_k^G + \sum_{k=i}^{j} L_k^O).$$

We want to obtain a paving that will minimize the total increase in area. This is consistent with the usual manufacturing requirement of minimizing the material usage, and the design objective of minimal wrinkling. The problem can be formulated as:

$$x_{i,j} = \begin{cases} 1, & if\ the\ i-th\ stripe\ is\ in\ the\ same\ paving\ with\ the\ j-th \\ 0, & otherwise \end{cases}$$

$$\boldsymbol{min} \sum_{i=0}^{n-1} \sum_{j=i}^{n-1} F_{ij} x_{i,j}$$

subject to:

$$\sum_{i=0}^{n-1} x_{i,j} \le 1, \qquad (j=0,1,\ldots,n)$$

$$\sum_{j=0}^{n-1} x_{i,j} \le 1, \qquad (i=0,1,\ldots,n);$$

the number of wrinkles w is given by $w = \sum_{i=0}^{n-1} \sum_{j=i}^{n-1} x_{i,j}$.

Thus $x_{0,1} = 1$ means the first two stripes will be combined to form one wrinkle, and $x_{2,4} = 1$ indicates another wrinkle occupying 3rd – 5th stripes. Note that some additional material (which accounts for the extra area of the wrinkled stripe over the area of the original surface) can only enter into the model from the two ends. Also, the first/last stripe must behave as the begin/end of a single paving (respectively). So $\sum_{j=0}^{n-1} x_{0,j} = 1$ and $\sum_{i=0}^{n-1} x_{i,n-1} = 1$. Since the regions are continuous, the j-th stripe is at the end of one region, and the $(j+1)$-th stripe begins at the next paving. Thus $\sum_{k=j+1}^{n-1} x_{j+1,k} - x_{i,j} = 0$. Finally, the material properties should also play a role in the wrinkling: stiff materials form fewer wrinkles of larger size, while soft materials form more but smaller wrinkles when draped over the same mold. We incorporate this into the model by setting a parameter, called the threshold energy, $K^*_{Threshold}$, which is incorporated into the model as: $(K_{ij}^* - m)x_{i,j} + m \ge K_{Threshold}^*$, where $K^*_{Threshold}$ is the minimum value of K^* in a paving from the i-th to the j-th stripes and m is a large number. Thus $K_{ij}^* \ge K_{Threshold}^*$, when $x_{i,j} = 1$, i.e., there is a paving, and K_{ij}^* is unconstrained when $x_{i,j} = 0$. In all, the entire energy minimization model is formulated as:

$$\boldsymbol{min} \sum_{i=0}^{n-1} \sum_{j=i}^{n-1} F_{ij} x_{i,j}$$

subject to:

$$\sum_{i=0}^{n-1} x_{i,j} \le 1,$$

$$\sum_{j=0}^{n-1} x_{i,j} \le 1,$$

$$\sum_{k=j+1}^{n-1} x_{j+1,k} - x_{i,j} = 0$$

$$(K_{ij}^* - m)x_{i,j} + m \ge K_{Threshold}^*$$

for i = 0, …, n-1 and j = 0, …, n-1

Note that we can re-formulate the above IP with much fewer variables, but the resulting model would become non-linear. Since the solver must be linked to a solid modeling system which outputs the parameter values, we

implemented a simulated annealing method using Visual C++ to solve this system. The solver is linked using API facilities to our commercial CAD system, Solidworks™. For brevity, the details of the solver are omitted here.

4.3 Examples

In this section, we present a few simple examples to demonstrate the energy based model. Figure 13 shows our standard test part, a mold of an ellipsoidal shape. The resulting wrinkles are visually similar to those generated for a physical sample (c.f. Figure 3c). The second example shows a region on the upper surface of a ladies shoe last. The green line is the generator curve, and the light white lines show the geodesic curves forming the stripes. Using two different values of K^*, different wrinkle geometry is obtained as shown in Figure 14.

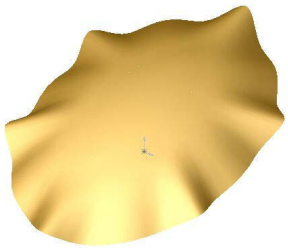

Figure 13. Wrinkles on an ellipsoid

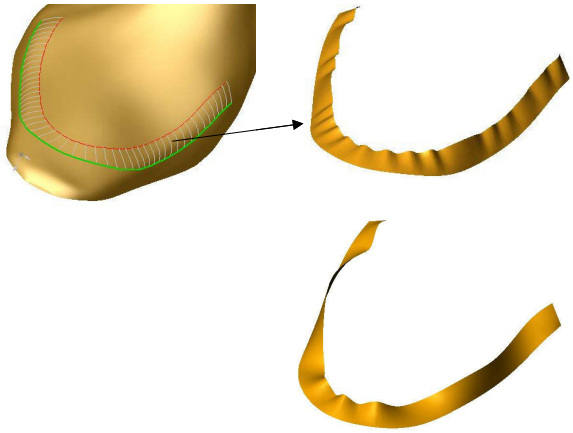

Fig. 14. Part of a shoe last surface with energy-based wrinkles, $K^* = 0.05$ *(top)* and $K^* = 0.2$

Another example was constructed by simulating the process of wrapping the rim between the upper and the bottom surfaces of a shoe last (see Figure 15).

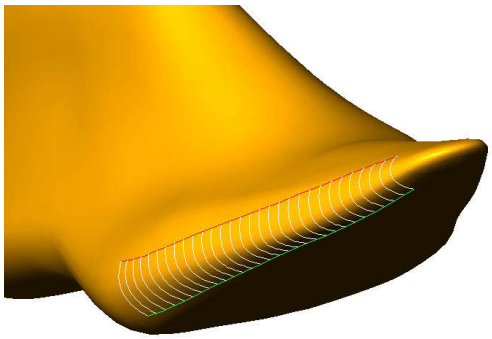

Fig. 15. Wrapping the rim of a shoe last

Although the portion we are interested in is wrinkling on the bottom surface (the upper surface will be ironed), some neighboring portion on the upper surface will also contribute some energy. In this example, the generator curve is shown in red, and the offset curve in green, using 31 geodesics to generate 30 stripes. Two wrinkled patches are constructed with $K^*_{Threshold} = 0.2$ resulting in 3 wrinkles (6 pavings) and $K^*_{Threshold} = 0.1$ resulting in 4.5 wrinkles. The corresponding wrinkled surfaces are shown in isolation in Figure 16(a) and (b).

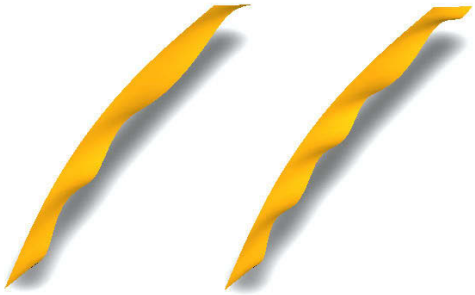

(a) $K^*_{Threshold} = 0.2$(b) $K^*_{Threshold} = 0.1$

Fig. 16. Wrinkled patch on bottom surface

5. SUMMARY

This paper concerns with the generation of wrinkled geometries on smooth parametric surfaces. Using traditional descriptors for wrinkle geometry and some experimental studies in footwear design, we defined a simple parametric form to define wrinkle shapes; the parameters control the wrinkle boundary; geodesic offsets are used for defining the wrinkle extent. Two wrinkle operators were developed. The first one allows the user to completely define the parameter values and control the wrinkle geometry. An application in the design of footwear was demonstrated. The second operator uses an optimization model that minimizes the

total (extra) material required to cover a given non-developable region by a flexible, wrinkled form. Again, the motivation of this operator is from practical requirements in the footwear manufacture when the objective is to minimize the area of the pattern used to cover some region on a shoe last.

6. ACKNOWLEDGEMENTS

The authors would like to thank Northford Mfg Ltd., Effect Group Ltd. for their support. Part of the research was supported by the RGC CERG (grant HKUST6235/02E).

7. REFERENCES

[1] Ng, H. N., Grimsdale, R. L., "Computer Graphics Techniques for Modeling Clothes," IEEE Computer Graphics and Applications, Computer Graphics in Textiles and Apparel, p 28-41, Sept 1996.

[2] Aono M., "A Wrinkle propagation model for cloth," CG International, Computer Graphics Around the World, Springer-Verlag, p 95-115, 1990.

[3] Aono M, Breen DE, Wozny MJ, "Modeling methods for the design of 3D broadcloth composite parts," Computer-Aided Design, v 33, n 13, p 989-1007, Nov 2001.

[4] Kunii TL, Gotoda H., "Singularity theoretical modelling and animation of garment wrinkle formation processes," Visual Computer, v 6, n 6, p 326-36, 1990.

[5] Fan, J., Wang, Q., Yuen, M.-F., Chan, C. C., "A Spring-mass Model-Based Approach for Wrapping Cloth Patterns on 3D Objects," The Journal of Visualization and Computer Animation, v 9, p 215-227, 1998.

[6] Singh, K, Fiume, E., "Wires: a Geometric Deformation Technique," Computer Graphics Proceedings, Annual Conference Series, 1998, ACM SIGGRAPH, p 405-414.

[7] Kim, K. J., Lee, I. K., "The Perspective Silhouette of a Canal Surface," Computer Graphics Forum, v 22, n 1, p 15-22, 2003.

[8] Piegl, L. A., Tiller, W., "Computing Offsets of NURBS curves and Surfaces," Computer-Aided Design, v 31, p 147-156, 1999.

[9] Azariadis, P. N., Aspragathos, N. A., "Geodesic Curvature Preservation in Surface Flattening Through Constrained Global Optimization," Computer-Aided Design, v 33, p 581-591, 2000.

[10] McCartney, J., Hinds, B. K., Seow, B. L., "The flattening of triangulated surfaces incorporating darts and gussets," Computer-Aided Design, v 31, 249-260, 1999.

[11] Hoschek, J., "Approximation of surfaces of revolution by developable surfaces," Computer-Aided Design, v 30, n 10, p 757-763, 1998.

[12] Do Carmo, M., Differential geometry of curves and surfaces, Englewood Cliffs, NJ: Prentice-Hall, 1976.

[13] Wolter, F.-E., Friese, K.-I., "Local & Global Geometric Methods for Analysis Interrogation, Reconstruction, Modification & Design of Shape," Procs of Computer Graphics Intl 2000, Geneva, IEEE, June 2000.

[14] Kimmel, R., Amir, A., Bruckstein, A. M., "Finding shortest paths on surfaces," Curves and Surfaces in Geometric Design, edited by Laurent, Le. Méhauté and Schumaker, p 259-268, Aug 1994.

[15] Kanai, T., Suzuki, H., "Approximate Shortest Path on a Polyhedral Surface and its Applications," Computer-Aided Design, v 33, p 801-811, 2001.

[16] Maekawa, T., "Computation of Shortest paths on Free-Form Parametric Surfaces," ASME Journal of Mechanical Design, v 118, p 499-508, Dec 1996.

[17] Piegl L, Tiller W, The NURBS book, 2nd ed, Springer, New York, 1997.

[18] Hadenfeld, J., "Local Energy Fairing of B-Spline Surfaces," Mathematical Methods in CAGD III, ed. M. Daehlen, T. Lyche, and L. L. Schumaker, p 1-10, 1995.